SCIENCE CHINA
Information Sciences

• LETTER •

November 2024, Vol. 67, Iss. 11, 219401:1–219401:2
https://doi.org/10.1007/s11432-024-4138-8

# Tunable lithium niobate metasurfaces for phase-only modulation based on quasi-bound states in the continuum

Ruoying KANYANG[1,2], Cizhe FANG[1,2*], Yibo WANG[1,2], Xiaoxi LI[1,2], Xiangyu ZENG[1,2], Yan LIU[1,2], Yue HAO[1,2] & Genquan HAN[1,2]

[1]*School of Microelectronics, Xidian University, Xi'an* 710071*, China;*
[2]*Hangzhou Institute of Technology, Xidian University, Hangzhou* 311200*, China*

Received 22 April 2024/Revised 26 June 2024/Accepted 21 August 2024/Published online 12 October 2024

Tunable Huygens' metasurfaces possess almost arbitrary control over the wavefront, enabling engineered refraction, deflection, focusing, and polarization control in optical systems [1]. However, phase-only modulation remains challenging due to the strong mode loss [2]. The concept of bound states in the continuum (BICs) has been shown to serve as an intriguing interference mechanism for suppressing radiation loss [3]. The combination of BICs and Huygens' regime offers possibilities to optimize the performance of tunable Huygens' metasurface [4]. Compared with different modulation means, electrostatic biasing is of particular interest for its continuous tunability, high-speed modulation, and low power consumption [5].

Here, an electro-tunable $LiNbO_3$ metasurface is proposed to achieve phase-only modulation. We use the finite element method to thoroughly investigate the optical properties of the structure by analyzing the transmission spectrum, electric/magnetic field distribution, and multipole decomposition. By optimizing the dimensions of the structure, we have established the Huygens' BIC regime. This extreme Huygens' metasurface offers $2\pi$ phase modulation while maintaining near-full transmission amplitude. The proposed structure holds the potential to greatly enrich the applicability and practicality of the $LiNbO_3$ metasurface.

*Design and Discussion.* The single unit of the proposed $LiNbO_3$ metasurface is shown in Figure 1(a). The elliptical cylinders are hosted on a glass substrate. To facilitate the voltage bias, thin nanobars serving as biasing lines are introduced to connect the elliptical cylinders. The inclination angle between the long axis of the elliptical cylinder and the $y$-axis is denoted by $\theta$. The height, length of the long axis and short axis of the elliptical cylinder, and width of the basing line are denoted by $h_{\mathrm{LiNbO_3}}, a, b$, and $w$, respectively. The symbols $p_x$ and $p_y$ represent the period along the $x$ and $y$ axes, respectively. The Huygens' metasurface is excited by the transverse electric (TE) polarized wave propagating along the $z$-axis. A $z$-cut $LiNbO_3$ is adopted in the simulation. The refractive index of $LiNbO_3$ is set as $n_x = n_y = n_o = 2.21$ and $n_z = n_e = 2.14$, while the refractive index of glass is set as 1.5. Indium-tin-oxide (ITO) layers with an ultrathin thickness of 10 nm are integrated as electrodes at the top and bottom of the $LiNbO_3$ elliptical cylinders to control the Huygens' metasurface electrically. The initial values of $p_x$, $p_y$, $h_{\mathrm{LiNbO_3}}, w, a$, and $b$ are set as 650, 1022, 800, 30, 350, and 160 nm, respectively.

Figure 1(b) depicts the band structures at $\theta = 0°$ along the $\Gamma$-$X$ direction. Two robust modes exist above the lightline. The Q factors of those modes with different inclination angles $\theta$ are depicted in Figure 1(c). The Q factors of the two modes are infinite at $\theta = 0°$ and decrease asymptotically with the increase in $\theta$. These two modes exist above the lightline and possess infinite Q factors, indicating that they are BIC resonant modes. The relationship between Q and the asymmetry parameters $\alpha$ can be expressed as $Q \propto \alpha^{-2}$, in which $\alpha$ is defined as $\alpha = \sin\theta$, where $-2$ is the slope of the fitting line. This is the universal property of the symmetric-protected BICs. Due to the vanishing of the coupling constants with all radiating waves, the ideal BIC resonant mode does not radiate. Upon distorting the in-plane symmetry, the ideal BIC transforms into the leaky mode with a finite Q factor. The transmission amplitude at $\theta = 0°$, $5°$, and $10°$ are depicted in Figure 1(d). The introduction of $\theta$ collapses the ideal BIC into two QBICs resulting in the emergence of two dips in the transmission spectrum.

To shed light on the multipole contribution of the two QBICs, the calculated results are shown in Figure 1(e). The details of the multipole decomposition can be found in Appendix A. The electric dipole contributes to the scattering peak located at 1484 nm, while the scattering peak located at 1494 nm mainly results from the magnetic dipole. They are identified as the electric-QBIC mode (E-QBIC) and magnetic-QBIC (M-QBIC), respectively. The electric and magnetic field profiles of those QBICs are demonstrated in Figure 1(f), respectively. The electric and magnetic fields of those QBICs manifest the generation of the electric/magnetic polarization along the long/short axis of the elliptical cylinders of the E-QBIC/M-QBIC, respectively. The symmetry properties of those two QBICs are discussed in Appendix B.

We have changed the incident wavelength $\lambda$ and inclination angles $\theta$ to scrutinize the variation in transmission am-

* Corresponding author (email: fangcizhe@xidian.edu.cn)

 

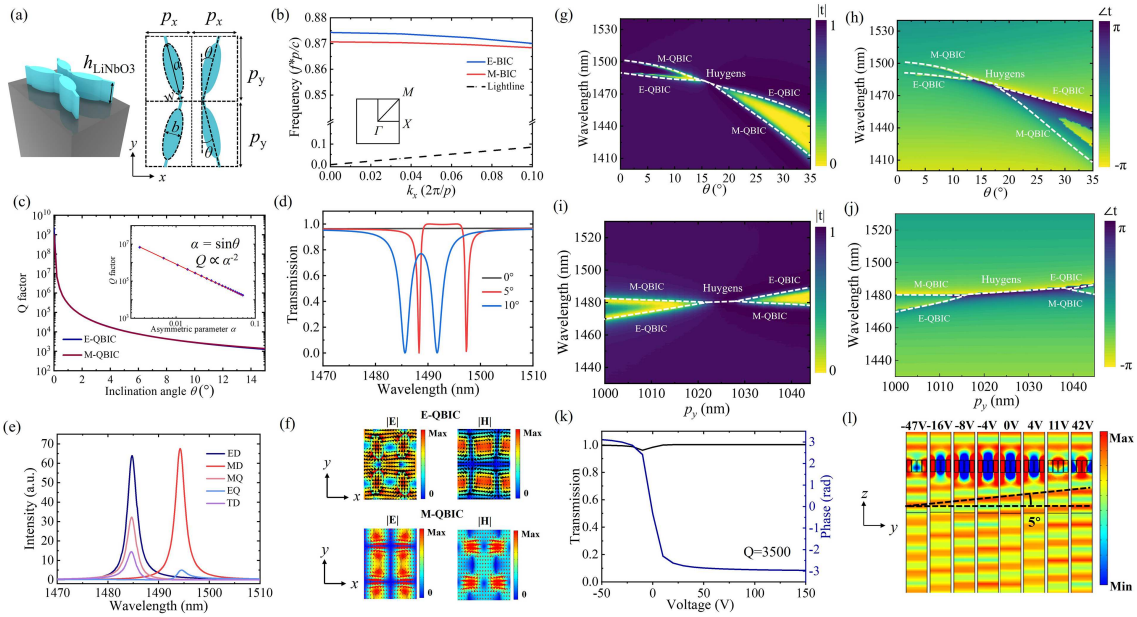


**Figure 1** (Color online) (a) Sketch of the $LiNbO_3$ metasurface. (b) The band structure of the $LiNbO_3$ metasurface. (c) The dependence of the Q factor on the inclination angle $\theta$. (d) The transmission amplitude for different $\theta$. (e) The scattering energy as a function of wavelength with $\theta = 10°$. (f) The electric field and magnetic field profiles of E-QBIC and M-QBIC. Calculated transmission amplitude (g) and phase (h) as functions of $\lambda$ and $\theta$. $|t|$ and $\angle t$ represent the transmission amplitude and phase, respectively. Calculated transmission amplitude (i) and phase (j) as functions of the $\lambda$ and $p_y$. (k) The transmission and phase spectra as functions of the applied voltage at $\lambda$=1463 nm. (l) Electric field profiles of the metasurface in the $y$-$z$ plane for different applied biases.

plitude and phase of those E-QBIC and M-QBIC. As shown in Figures 1 (g) and (h). The two QBICs cross each other as the $\theta$ varies, giving rise to an overlapped spectral domain at $\theta = 17°$. This spectrally overlapped regime is crucial to achieving the satisfaction of Huygens' regime. Considering the practical application, it is necessary to obtain the Huygens' regime without dramatically affecting the Q factor. We fix the $\theta$ at 16°. As shown in Figures 1 (i) and (j), utilizing the different sensitivities of both QBICs to the variation of $p_y$, the Huygens' BIC can be attained by just adjusting $p_y$. The significant sensitivity of E-QBICs to $p_y$ is attributed to the electric polarization in adjacent elliptical cylinders aligned along the $y$-axis.

*Tunable Huygens' BIC metasurface.* The phase-only modulation is highly promising for dynamic applications. To support the electro-optical tuning, a bias voltage is applied to the $LiNbO_3$ metasurface. The $LiNbO_3$ metasurface is operated at the Huygens' regime, where the Huygens' mode is detuned via electro-refraction induced in the $LiNbO_3$. The details of electrical modulation can be found in Appendix C. A nearly $2\pi$ phase modulation and near-unity transmission amplitude are obtained with the applied bias increases from $-50$ V to 150V as shown in Figure 1(k). To demonstrate the wavefront phase manipulation of the transmitted light, we have plotted the electric field in the $y$-$z$ plane crossing the middle of the $LiNbO_3$ elliptical cylinders under different voltages. As shown in Figure 1(l). The transmission amplitude/phase changes of the structures are 1/345°, 0.99/302°, 0.99/255°, 1/212°, 0.98/161°, 0.96/118°, 0.96/76°, and 0.99/30° under the different voltage bias at $-47$, $-16$, $-8$, $-4$, 0, 4, 11, and 42 V. The bending angle of the wavefront is around 5°, which satisfies the generalized Snell's law.

*Conclusions.* We have proposed and theoretically analyzed an electro-tunable extreme Huygens' BIC metasurface consisting of $LiNbO_3$ elliptical cylinders. After optimizing the geometry parameter of the structure, we have realized over $2\pi$ phase retardation of transmitted light while maintaining over 96% transmission amplitude. The metasurface can be continuously tuned based on the EO property of the $LiNbO_3$ without a drastic change in the transmission. The proposed $LiNbO_3$ metasurface will be a good candidate for developing reconfigurable optical components in optical wavefront shaping, displaying, and other applications.

**Acknowledgements** This work was supported by National Key R&D Program of China (Grant No. 2023YFB4402303), National Natural Science Foundation of China (Grant Nos. 62090033, 92364204, 92264202), the Major Program of Zhejiang Natural Science Foundation (Grant No. LDT23F04024F04), the Fundamental Research Funds for the Central Universities (Grant No. XJSJ24088), and the Postdoctoral Fellowship Program of Shaanxi Province (Grant No. 2023BSHEDZZ182).

**Supporting information** Appendixes A–C. The supporting information is available online at info.scichina.com and link.springer.com. The supporting materials are published as submitted, without typesetting or editing. The responsibility for scientific accuracy and content remains entirely with the authors.

**References**

1 Wang Y, Fan Q, Xu T. Design of high efficiency achromatic metalens with large operation bandwidth using bilayer architecture. Opto-Electron Adv, 2021, 4: 200008
2 Liu C, Chen L, Wu T, et al. All-dielectric three-element transmissive Huygens' metasurface performing anomalous refraction. Photon Res, 2019, 7: 1501
3 Koshelev K, Lepeshov S, Liu M, et al. Asymmetric metasurfaces with high-Q resonances governed by bound states in the continuum. Phys Rev Lett, 2018, 121: 193903
4 Liu M, Choi D. Y. Extreme Huygens' metasurfaces based on quasi-bound states in the continuum. Nano Lett, 2018, 18: 8062–8069
5 Gao B, Ren M, Wu W, et al. Electro-optic lithium niobate metasurfaces. Sci China Phys Mechan Astron, 2021, 64: 240362